Ruthenium(II) Tris(bipyridine)-Centered Poly(ethylenimine) for Gene Delivery

Gina L. Fiore,[†] James M. Edwards,[‡] Sarah J. Payne,[†] Jessica L. Klinkenberg,[†] Daniel G. Gioeli,[‡] J. N. Demas,[†] and Cassandra L. Fraser*,[†]

Department of Chemistry, University of Virginia, McCormick Road, P.O. Box 400319, Charlottesville, Virginia 22904, and Department of Microbiology and Cancer Center, University of Virginia, 1300 Jefferson Park Avenue, P.O. Box 800734, Charlottesville, Virginia 22908

Received May 1, 2007; Revised Manuscript Received May 31, 2007

Ruthenium(II) tris(bipyridine)-centered poly(ethylenimine) (Ru PEI) was synthesized via acid hydrolysis of Ru tris(bipyridine)-centered poly(2-ethyl-2-oxazoline) (Ru PEOX), and the luminescence, DNA entrapment, and transfection efficiencies were evaluated. Emission maxima for Ru PEI samples are red-shifted compared to Ru PEOX precursors, and the luminescence lifetimes are shorter in both methanol and aqueous solutions. Slower oxygen quenching of Ru PEOX and Ru PEI luminescence versus $[Ru(bpy)_3]Cl_2$ (bpy = bipyridine) is attributed to polymer shielding effects. Ru PEI luminescence is similar in the presence and absence of DNA. Ru PEI (7900 Da) and linear PEI (L-PEI; 22 000 Da) fully entrapped DNA (5.4 kb; pcDNA) at an N/P ratio of 2. LNCaP prostate cancer cells were transfected with a plasmid encoding for green fluorescent protein using Ru PEI and L-PEI vectors for comparison. For N/P = 48, the transfection efficiency for Ru PEI was ∼50% relative to that of L-PEI.

Introduction

Polymer vectors have become increasingly important as alternatives to viral gene delivery systems, which have associated safety risks and high costs.[1−3] Nonviral vectors may be tuned to specific therapeutic needs via synthesis and materials processing. Current research focuses on degradable vectors incorporating features designed to overcome particular obstacles in the delivery process, such as DNA stability, targeting and internalization,[4−9] endosomal disruption,[10,11] dissociation of the DNA from the polymer,[12,13] and nuclear localization.[11] For example, targeting groups (i.e., folic acid,[4,5] antibodies,[6,7] and antibody fragments[8,9]) and labile linkages[3,14−16] have been incorporated into delivery systems to increase specificity and facilitate degradation and timely DNA dissociation from the cationic polymer matrix. Additionally, delivery vectors are often combined with other polymers, such as poly(ethylene glycol) (PEG), to increase solubility and circulation while also decreasing the toxicity of the associated materials.[14,16−18]

Poly(ethylenimine) (PEI), a polycationic polymer that electrostatically binds and protects DNA, is common in gene delivery.[17,19−21] PEI also has a large buffering capacity due to the many secondary amines along the polymer backbone that can become protonated at physiological and acidic pHs, thus acting as a "proton sponge."[19,22−24] PEI has been synthesized by two general methods that produce branched or linear polymers. Branched materials are made by the acid-catalyzed ring-opening polymerization of aziridine.[25−27] By controlling the reaction conditions, low to high degrees of branching can be achieved.[26] Alternatively, linear PEI (L-PEI) is synthesized by the hydrolysis or reduction of amide side chains in polyoxazoline precursors.[28−30] The degree of hydrolysis can be controlled by the concentration of acid or base, as well as the reaction time.[29,30] By varying the number of initiation sites, poly(2-ethyl-2-oxazoline) (PEOX) star polymers have also been synthesized, and subsequent acid hydrolysis produced star PEI hydrogels.[31]

Molecular architecture and size can affect toxicity and transfection efficiency.[17,19,21,32] For instance, linear systems have shown higher transfection efficiencies[33] and lower associated toxicities compared to branched systems.[14] Lower molecular weight PEI is generally less toxic; however, transfection also decreases with decreasing molecular weight.[34] Toxicity has also been addressed by the incorporation of degradable linkages.[3,14,15,35] To take advantage of these factors, acid-labile imine linkages have been incorporated into PEI to create high molecular weight polymers that will degrade into nontoxic smaller fragments in the acidic environments of endosomes. The transfection efficiencies of acid-labile PEIs were found to be comparable to that of PEI, but toxicities were lower.[15] The incorporation of PEG is also beneficial for PEI delivery systems.[14,18,27,36] Similar transfection efficiencies but lower cytotoxicities have been noted for PEG-grafted PEI,[36] and DNA condensation is also enhanced for PEI−PEG block copolymers[27,36] compared to unmodified PEI.

Polymeric metal complexes (PMCs) offer some attractive features for delivery vectors. Made by controlled polymerization and modular metal template approaches, systematic variation of molecular weights, compositions, and architectures is possible, which is important for structure−activity studies and properties optimization.[37−40] Furthermore, since metals can sense and respond to stimuli with concomitant structural and property changes, appropriately designed complexes could play a role in vector degradation or report on the location and surroundings of the polymer at different stages in the delivery process. As a first step in testing the feasibility of this concept and an initial model for incorporating a responsive metal into polymeric gene delivery vector materials, we explored the synthesis, luminescence, DNA entrapment, and gene transfection of six-arm star-shaped ruthenium tris(bipyridine)-centered PEI (Ru

* To whom correspondence should be addressed. E-mail: fraser@virginia.edu.
[†] Department of Chemistry.
[‡] Department of Microbiology and Cancer Center.

10.1021/bm700481h CCC: $37.00
Published on Web 07/31/2007

PEI). This synthetic target is accessible via ruthenium tris-(bipyridine)-centered PEOX (Ru PEOX), one of the first PMC systems reported by our group.[41−43] Ultimately, PMC materials can be adapted and elaborated on the basis of the growing body of knowledge of vector optimization. Structural and physical properties of the metal complex could be tuned to dissociate macroligands and exhibit differential responses during specific steps in the gene delivery process.

Experimental Section

Materials. The metalloinitiator, $[Ru\{bpy(CH_2Cl)_2\}_3](PF_6)_2$,[44] and $bpyPEOX_2$[45,46] macroligands were prepared by previously reported methods. 2-Ethyl-2-oxazoline (Aldrich) was dried over CaH_2 and distilled prior to use. Acetonitrile (Fisher) was purified by passage through alumina columns.[47] $[Ru(bpy)_3]Cl_2$ was obtained from GFS Chemicals. L-PEI (ExGen 500, 22 kDa) was obtained from Fermentas. The expression vector, pcDNA3.1 (5.4 kb), was obtained from Invitrogen, and the green fluorescent protein plasmid (pGFP) was obtained from Clontech. LNCaP cells were a gift from L. W. K. Chung. All other reagents and solvents were used as received.

Methods. ^{1}H NMR (300 MHz) spectra were recorded on a Varian UnityInova 300 spectrometer in $CDCl_3$. Resonances were referenced to the signal for residual chloroform at 7.26 ppm. UV−vis spectra were obtained on a Hewlett-Packard 8452A diode array spectrophotometer. Molecular weights were determined by gel permeation chromatography (GPC) in dimethylformamide (DMF) containing 0.4% Et_3N at 50 °C versus poly(methyl methacrylate) (PMMA) standards using refractive index and diode array UV−vis detection. Polymer Labs 5 μm mixed C columns along with Wyatt Technology Corporation (Optilab-DSP Interferometric Refractometer) and Agilent and Hewlett Packard (series 1100) HPLC instrumentation were used in GPC analysis. Excitation and emission spectra were recorded on a SPEX Fluorolog 1680 using right-angle illumination. Correction factors were applied to emission spectra to compensate for photomultiplier tube efficiencies at different wavelengths. Lifetimes were measured using a VSL-337 pulsed nitrogen laser (λ = 337 nm) (Laser Science, Inc., Franklin, MA) for optically dilute solutions (A < 0.2). The luminescence signal was detected with a photomultiplier tube viewed on a 500 MHz TDS 540 digital oscilloscope (Tektronix, Inc., Beaverton, OR), and transferred to an interfaced PC. Instrumentation was controlled by a Labview program. Data were fit to a single, double, or triple exponential decay using a Marquardt algorithm. Methods and instrumentation for the gel retardation assay and transfection of LNCaP cells are described in the respective sections below.

$[Ru(bpyPEOX_2)_3]^{2+}$. Six-arm star-shaped Ru PEOX precursors were prepared by reported methods.[42] ^{1}H NMR (300 MHz, $CDCl_3$): δ 3.2−3.6 (br m, −(NHCH_2CH_2)−), 2.1−2.5 (br m, −(C(O)CH_2CH$_3$)−), 1.0−1.4 (br m, −(C(O)CH$_2$CH_3). GPC: M_n = 16 800, polydispersity index (PDI) = 1.13; M_n = 14 200, PDI = 1.20; M_n = 11 100, PDI = 1.11.

$[Ru(bpyPEI_2)_3]^{2+}$. A representative procedure is provided. Amide hydrolysis of Ru PEOX was performed by the method of Brissault et al.[29] with the following modifications: $[Ru(bpyPEOX_2)_3]^{2+}$ (102 mg, M_n = 11 100) was dissolved in H_2O (6.5 mL), and concentrated HCl (8.5 mL) was added. The mixture was heated at reflux for 4 h, cooled to 25 °C, and dried in vacuo. The orange solid was dissolved in a minimal amount of H_2O, and 3 M NaOH was added until pH 10 was reached. The suspension was centrifuged, the supernatant was decanted, and the resulting orange precipitate was dried in vacuo. The crude polymer product was dissolved in CH_2Cl_2 and separated from residual salts via cannula filtration. The solution was dried over Na_2SO_4, cannula filtered, and concentrated in vacuo to produce a dark red tacky product (97% hydrolyzed): 48 mg (98%). ^{1}H NMR ($CDCl_3$, 300 MHz): δ 3.4−3.5 (m, −N(COCH$_2$CH$_3$)CH_2CH_2−), 2.6−3.2 (m, −NHCH_2CH_2−), 2.4 (q, −N(COCH_2CH$_3$)−), 1.1 (t, −N(CO-CH$_2$CH_3)−). M_n (NMR) = 5400.

$[Ru(bpy)_2(bpyPEOX_2)]^{2+}$. Macroligand chelation was performed as previously reported,[48] but using CH_3OH as the solvent and drying over Na_2SO_4, with the following reagent loadings and conditions: $Ru(bpy)_2Cl_2\cdot 2H_2O$ (9.9 mg, 0.020 mmol), CH_3OH (5 mL), $AgPF_6$ (17.9 mg, 0.071 mmol), $bpyPEOX_2$ (51.9 mg, 0.003 mmol, 15 700 Da), 4 d reflux. The reaction product was analyzed by GPC with inline UV−vis diode array detection.

Luminescence. Lifetime data were acquired at room temperature (~22 °C) for solutions purged with nitrogen, air (21% oxygen), or pure oxygen. All decay curves could be fit to a double- or triple-exponential equation:

$$D(t) = \sum_{j=1}^{N} \alpha_j \exp(-t/\tau_j),\ N = 2,3 \tag{1}$$

where the α and τ values were measured by fitting the decay data to sums of exponentials using a Marquardt nonlinear least-squares algorithm. Lifetimes are reported as pre-exponential weighted lifetimes determined from[49]

$$\tau_{pe} = \sum_{j=1}^{3} \alpha_j \tau_j / \sum_{j=1}^{3} \alpha_j \tag{2}$$

Oxygen is a dynamic or collisional quencher of the complexes. In solution, the dependence of emission intensity and lifetime with quencher concentration is given by the Stern−Volmer equations:[50]

$$I_0/I = 1 + K_{SV}[Q] \tag{3a}$$

$$\tau_0/\tau = 1 + K_{SV}[Q] \tag{3b}$$

$$K_{SV} = k_q \tau_0 \tag{3c}$$

where the I values are emission intensities, the τ values are lifetimes, K_{SV} is the Stern−Volmer quenching constant, and k_q is the bimolecular rate constant for quenching of the excited state. The subscript 0 denotes the value of the quantity in the absence of the quencher. The Stern−Volmer constants were determined by linear regression of Stern−Volmer plots.

Gel Shift Assay. The PEI−DNA complexes were prepared using pcDNA3.1 with L-PEI (22 000 Da) and Ru PEI (M_n = 5400, 6700, or 7900) by the method of Boussif et al.[22] The PEI nitrogen to DNA phosphate (N/P) ratio calculation assumes that 1 μg of DNA contains 3 nmol of phosphate and 1 μL of PEI stock solution (22 000 Da, 10 μM) contains 5.47 nmol of amine nitrogens. Ru PEI calculations were performed similarly. Because of limited aqueous solubility, the Ru PEI was dissolved in CH_3OH to create a 0.3 M stock solution and then diluted with water to a final concentration of 300 μM. A stock solution of DNA (2 μg, 6 nmol phosphate in 10 mM Tris buffer) was gently mixed with 150 mM NaCl solution (15 μL). Separate aqueous solutions of L-PEI (2 nmol of nitrogen) and Ru PEI (2, 6, 9, and 12 nmol of nitrogen) samples were prepared. The PEI solutions (300 μM to 12 mM) were added to aliquots of the DNA solution (875 ng, 300 μM) to create the desired N/P ratios, followed by vigorous mixing. The PEI−DNA complexes were diluted in DNA loading buffer (3.33 μL) containing 10 mM Tris pH 7.5, 0.25% bromophenol blue and xylene cyanol, and 40% w/v sucrose. The PEI−DNA complexes were run on a 0.7% agarose gel in Tris buffer containing ethidium bromide (5 μg/mL) and visualized with an Alpha Innotech gel/blot reader.

Transfection. LNCaP cells were maintained in T-medium with 5% non-heat-inactivated fetal bovine serum (NHI-FBS) at 37 °C in a humidified chamber. Cells were seeded at 2.0×10^5 cells per well in six well plates and allowed to adhere for 48 h. The plasmid DNA (3 μg, pGFP in 10 mM Tris buffer) was combined with 150 mM NaCl (100 μL) and gently mixed. The PEI solutions (L-PEI or Ru PEI 7900 Da) were then added, and the resulting PEI−DNA transfection solutions were vigorously mixed. The PEI−DNA transfection solutions (200 μL

per well) were added to LNCaP cells in fresh T-medium (2 mL per well, 5% NHI-FBS). After 48 h, cells were fixed with paraformaldehyde (1.6 mL in 40 mL of phosphate-buffered saline) for 30 min and visualized using a Zeiss Axiovert 135 TV inverted microscope. The total cell number and number of fluorescent cells were determined from the average of three random independent visual fields under 40× magnification.

Results and Discussion

Polyoxazolines provide a facile route to PEI materials via hydrolysis or the reduction of amide functional groups. To test whether reported methods also extend to metallopolymers, $[Ru(bpyPEOX_2)_3]^{2+}$, with molecular weights ranging from 11 000 to 17 000 Da, was synthesized via a divergent metalloinitiation approach.[42] Hexafunctional $[Ru\{bpy(CH_2Cl)_2\}_3]^{2+}$ served as the initiator for the cationic ring-opening polymerization of 2-ethyl-2-oxazoline to produce orange glassy Ru PEOX materials with low polydispersity indices (PDI < 1.2). Due to the instability of $[Ru(bpy)_3]^{2+}$ under basic conditions, Ru PEOX six-arm stars were subjected to acid hydrolysis[29] with aqueous HCl to produce polycationic $[Ru(bpyPEI_2)_3]^{2+}$ products (Scheme 1). The solvent and volatile propionic acid byproducts were removed in vacuo, and the protonated polymers were treated with aqueous NaOH until pH 10 was achieved. Upon deprotonation of the polyammonium salt backbone (∼pH 9−10), the polymers precipitated out of solution due to the insolubility of neutral PEI in water.[51] After collection by centrifugation and drying under vacuum, Ru PEI products were dissolved in methylene chloride and filtered to separate from residual salts. This procedure provides dark red $[Ru(bpy)_3]^{2+}$-containing PEI materials and avoids high base concentrations and elevated temperatures that lead to purple byproducts, perhaps Ru bis(bpy) species.

Scheme 1. Synthesis of Ru PEOX and Ru PEI

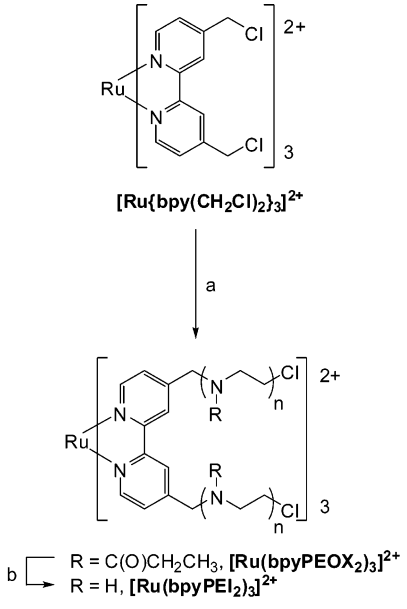

(a) EtOX, CH_3CN, 80 °C, ~2 d (b) aq HCl, 100 °C, 4 h

Molecular weights of the Ru PEOX precursors were determined by GPC in DMF containing 0.4% triethylamine relative to PMMA standards (Table 1). Because of the cationic nature of PEI and its tendency to interact with standard GPC columns, molecular weights for Ru PEI samples were instead analyzed by ^{1}H NMR by comparison with the respective Ru PEOX precursor. Because the bipyridine benzylic and aromatic peaks are not evident in ^{1}H NMR spectra,[42] molecular weights for Ru PEI were calculated based on the GPC M_n values for Ru PEOX and the relative integration of the peaks corresponding to the propanoyl side chains ($-N(COCH_2CH_3)-$) versus the PEI backbone methylene groups ($-NHCH_2CH_2-$) in hydrolyzed samples. For example, Ru PEOX (M_n (GPC) = 16 800 Da) yielded Ru PEI (97% hydrolysis; M_n (NMR) = 7900 Da) (Table 1). Ru PEOX materials with molecular weights up to ∼20 kDa are attainable via metalloinitiation,[42] leading to Ru PEI with molecular weights up to ∼10 kDa upon hydrolysis.

Table 1. Molecular Weight and UV−vis Spectroscopic Data for $[Ru(bpyPEOX_2)_3]^{2+}$ and Corresponding $[Ru(bpyPEI_2)_3]^{2+}$ Star Polymers

Ru PMC	M_n (kDa)	PDI[a]	DP_{arm}[c]	hydrolysis[d] (%)	λ_{abs}[e] (nm)	A[e]
PEOX	16.8[a]	1.13	27		461	0.350
PEI	7.9[b]			97	467	0.304
PEOX	14.2[a]	1.20	23		461	0.400
PEI	6.7[b]			97	466	0.238
PEOX	11.1[a]	1.11	18		461	0.459
PEI	5.4[b]			98	466	0.336

[a] Determined by GPC (DMF/0.4% Et_3N) vs linear PMMA standards. [b] Calculated from Ru PEOX M_n and % hydrolysis. [c] Degree of polymerization per arm of six-arm star. $DP_{arm} = DP_{star}/6$. [d] Determined by ^{1}H NMR via relative integration of $-NC(O)CH_2CH_3-$ and $-NHCH_2CH_2-$ resonances. [e] λ_{abs} = MLCT λ_{max} and A = absorbance for 0.10 mM CH_3OH solutions.

In an effort to access higher molecular weight Ru PEOX and thus, Ru PEI materials, a macroligand chelation approach was also explored. When PEOX is grown from an analogous iron metalloinitiator, $[Fe\{bpy(CH_2Cl)_2\}_3](PF_6)_2$, higher molecular weight star polymers (M_n ∼ 75 kDa) can be achieved. Here, iron serves as a protecting group for nucleophilic bpy centers, preventing coupling reactions with electrophilic initiating and propagating sites in oxazoline polymerizations.[46] Demetallation with aqueous base leads to $bpyPEOX_2$ macroligands up to ∼25 kDa in size, which can be resubmitted in chelation reactions with ruthenium reagents. As is illustrated by homopolymer and block copolymer ruthenium tris(bpy) polystyrenes with 1−6 arms,[37,48,52−56] dehalogenation of $Ru(bpy)_2Cl_2$ intermediates[48] and optimization of reaction conditions, including solvent, temperature, and time for different polymer compositions, are often required. To test this approach, $bpyPEOX_2$ macroligands (M_n = 12 800, 15 700, and 24 800) were synthesized via $[Fe(bpyPEOX_2)_3]^{2+}$ precursors for coordination reactions with ruthenium reagents. Initial efforts to generate $[Ru(bpy)_2(bpyPEOX_2)]^{2+}$ were modeled after previous work from our group;[37,48,52−56] however, attempts to produce $[Ru(bpy)_2(bpyPEOX_2)]^{2+}$ by dehalogenating $Ru(bpy)_2Cl_2$ with $AgPF_6$ in CH_3OH followed by the addition of $bpyPEOX_2$ were unsuccessful in both CH_3OH and DMF solutions.[48] After stirring for 4 days at reflux, GPC analysis with inline UV−vis diode array detection showed no evidence of Ru tris(bpy) chromophores associated with the eluting polymer peaks. Further optimization of the reaction conditions for PEOX is required for this alternative approach to be viable.

To evaluate the integrity of the Ru tris(bpy) center, Ru PEI and Ru PEOX were examined by UV−vis and luminescence spectroscopy. The nonpolymeric parent compound $[Ru(bpy)_3]^{2+}$ displays an absorption at λ_{abs} = 450 nm, characteristic of the metal-to-ligand charge transfer (MLCT) transition and an emission at λ_{em} = 612 nm in aqueous solution (in CH_3OH: λ_{abs} = 453 nm, λ_{em} = 615 nm).[57] Similar features are observed for Ru PEOX and Ru PEI as well (Table 1, Figure 1). However, the calculated extinction coefficient for Ru PEOX (e.g., 3500

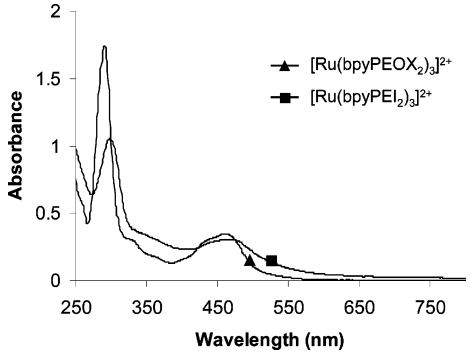

Figure 1. UV−vis spectra for Ru PEOX (▲) and Ru PEI (■) (0.1 mM in CH_3OH).

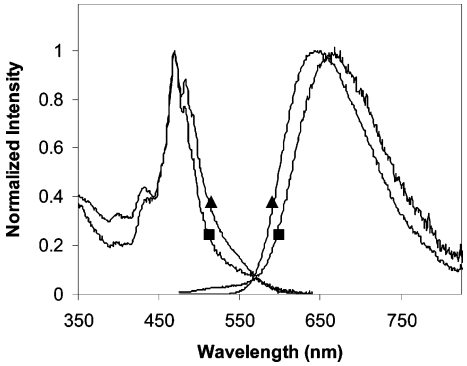

Figure 2. Excitation (left) and emission spectra (right) for Ru PEOX (14 200 Da) (▲) and Ru PEI (6700 Da) (■) in CH_3OH. Excitation scans were monitored at emission maxima (Ru PEOX: $\lambda_{em} = 649$ nm; Ru PEI: $\lambda_{em} = 674$ nm). Emission spectra were recorded after excitation at 461 nm.

M^{-1} cm^{-1}; 16 800 Da) is lower than that for $[Ru(bpy)_3]^{2+}$ (14 373 M^{-1} cm^{-1})[57] in methanol solution. Differences in the ϵ values may be due to error associated with polymer molecular weight determination, or alternatively, to partial degradation of the metal complex during polymer synthesis. The latter could also help to explain the ~20−25 kDa molecular weight limitation observed for Ru PEOX,[42] if byproducts react with the electrophilic propagating species to terminate the polymerization reaction prematurely. At the same concentration, absorbances for Ru PEI (0.304) are only slightly lower than those for Ru PEOX precursors (0.350) (Table 1), suggesting that the Ru tris(bpy) metal center was largely stable to the hydrolysis reaction conditions. The MLCT λ_{max} for Ru PEI (466 nm) is red-shifted compared to that for Ru PEOX (461 nm), and the absorbance band is broadened (Figure 1). Changes in the local environment attributable to the polyamine chains, partial degradation of the complex during acid hydrolysis or the basic workup, or a combination of these factors could be involved.

The luminescence properties of Ru PEOX and Ru PEI were investigated and compared with $[Ru(bpy)_3]^{2+}$ (Table 2). Although the excitation and emission spectra for Ru PEOX and Ru PEI are similar (Figure 2), Ru PEI luminescence spectra display a bathochromic shift in the emission in both methanol and aqueous solutions, with decreased intensities and shorter unquenched lifetimes, τ_0, (CH_3OH: 467 ns; H_2O: 328 ns) compared to those of Ru PEOX (CH_3OH: 838 ns; H_2O: 541 ns) and $[Ru(bpy)_3]^{2+}$ (CH_3OH: 785 ns; H_2O: 611 ns).[57] Similar and even more dramatic differences have been noted for nonpolymeric Ru(II) complexes with amine substituents directly attached to the bipyridine rings (versus Ru PEI with intervening methylene groups). For example, when $[Ru(bpy)_3]^{2+}$ was derivatized with diethylamino groups at the 4,4′ positions of the bipyridine ligands, red shifts in absorbance ($\lambda_{abs} = 518$ nm) and emission maxima ($\lambda_{em} = 700$ nm) and a shorter luminescence lifetime (130 ns) were observed in EtOH/CH_3OH (4:1) solution.[58] These differences may be explained by the energy gap law, which asserts that nonradiative processes can increase exponentially with decreases in energy between the ground and excited states.[59] These findings suggest that, for Ru PEI, substituent effects that shorten the lifetime dominate polymer shielding effects, which are known to lengthen luminescence lifetimes for Ru polypyridine complexes.[60,61]

Emission decay curves for Ru PEOX were fit with double exponentials and, for Ru PEI, were fit with triple exponentials. Preexponential weighted lifetimes are reported.[49] Multiexponential fits are not uncommon for polymers because of the presence of multiple microenvironments created by the polymer chains (e.g., different conformations, aggregation, surface vs interior sites).[62] Multiple luminophores can also give rise to multiexponential decay. The bimolecular oxygen quenching rate constants, k_q, for Ru PEOX and Ru PEI are less than those for $[Ru(bpy)_3]^{2+}$ (Table 2). As seen in dendrimer systems,[60] here too, the polymer chains can slow the diffusion of quencher to the metal center or shield it physically from contact with oxygen. Solvent effects are also noted through a comparison of k_q values; for all samples, luminescence is quenched more readily (i.e., k_q values are larger) in water than in CH_3OH. Plots of I_0/I and τ_0/τ versus oxygen concentration are linear with identical slopes equal to K_{SV} if there is a single class of luminophores that are all equally accessible to the quencher. Lifetime Stern−Volmer plots are linear for Ru PEOX and Ru PEI in aqueous solution. In methanol solution, the lifetime and intensity Stern−Volmer plots for Ru PEOX and Ru PEI were slightly downward curved, but in agreement with each other. This establishes that oxygen quenching is diffusional.[49] The complex decays and curved Stern−Volmer plots show that there is some heterogeneity in the environment of the luminescent Ru(II) chromophores. Such effects are well documented in both lifetime and intensity quenching data for oxygen sensors and polymeric systems.[62]

DNA entrapment and transfection were explored for Ru PEI and commercial L-PEI (22000 Da) for comparison. Plasmid DNA (pcDNA) was combined with Ru PEIs and L-PEI at various N/P ratios ranging from 1 to 4, and DNA−polymer complexes were analyzed by a gel retardation assay. Initial N/P

Table 2. Emission Maxima and Luminescence Lifetimes for $[Ru(bpyPEOX_2)_3]^{2+}$ and $[Ru(bpyPEI_2)_3]^{2+}$ Versus $[Ru(bpy)_3]^{2+}$ [a]

complex	M_n (Da)	solvent	λ_{em} (nm)	τ_0 (ns)	τ_{air} (ns)	τ_{O_2} (ns)	K_{SV} (M^{-1})	$k_q \times 10^{-9}$ (M^{-1} s^{-1})
$[Ru(bpy)_3]Cl_2$ [b]	641	CH_3OH	615	785	206	54	1881	2.4
		H_2O	612	611	391	167	2094	3.4
$[Ru(bpyPEOX_2)_3]^{2+}$ [c]	14 200	CH_3OH	649	838	312	105	708	0.8
	16 800	H_2O	636	541	460	296	652	1.2
$[Ru(bpyPEI_2)_3]^{2+}$ [d]	6700	CH_3OH	674	467	207	81	485	1.0
	7900	5% CH_3OH in H_2O	659	328	269	162	807	2.5

[a] $\lambda_{ex} = 461$ nm. [b] Lifetime data fit to single exponentials. [c] Lifetime data fit to double exponentials. Preexponential weighted lifetimes are reported. [d] Lifetime data fit to triple exponentials. Preexponential weighted lifetimes are reported.

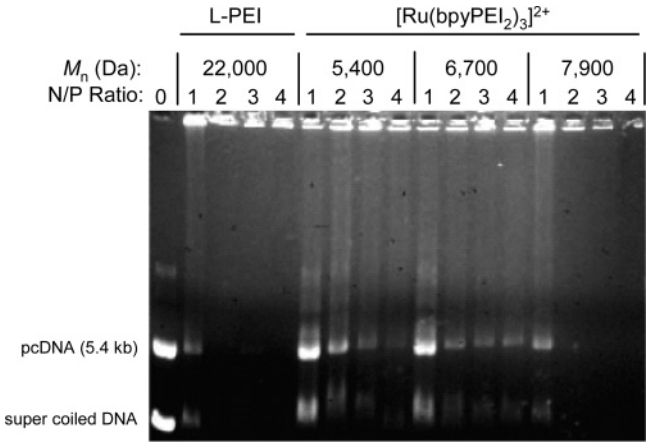

Figure 3. Gel retardation assay for L-PEI and Ru PEI complexes with pcDNA at various N/P ratios (N/P = 1−4). DNA was visualized with an ethidium bromide stain.

ratios were based on the report of Ferrari et al.[63] then adapted empirically for this study. When DNA is not fully entrapped by polymer chains, it can migrate down the agarose gel and thus be separated from PEI on the basis of size and charge. Because of the increase in size, full entrapment of DNA in PEI chains results in a complex that cannot migrate through the gel. Here, both Ru PEI (7900 Da) and L-PEI fully entrapped DNA at an N/P ratio of 2, whereas lower molecular weight Ru PEI (5400 and 6700 Da) did not fully entrap DNA even at an N/P ratio of 4 (Figure 3). It is possible, however, that low molecular weight Ru PEI vectors could effectively entrap DNA at higher N/P ratios. Ru PEI entrapped DNA and retarded migration through the gel at a significantly lower N/P ratio than previously reported for low molecular weight branched PEI (11 900 Da, N/P ratio = 27).[64] This may be attributed to an increase in secondary amines along the L-PEI chains of star Ru PEI versus a combination of secondary and tertiary amines in more highly branched systems.[17,29] Similar observations have also been noted by Brissault et al.[29] where L-PEI entrapped and transfected DNA more effectively than poly(*N*-propylethylenimine), an L-PEI with 3° amines along the polymer backbone. This argument is counterbalanced, however, by the increase in 1° amine terminal groups for branched PEI (vs star and linear), which often correlates with entrapment at lower N/P ratios.

The effects of DNA entrapment on Ru PEI luminescence were evaluated for aqueous solutions. As in methanol, Ru PEI (7900 Da) exhibited a bathochromic shift and shorter lifetime compared to Ru PEOX (16 800 Da) (Table 2). Ru PEI and DNA were combined in an N/P ratio of 2, the point at which DNA becomes fully entrapped in the PEI chains. Emission spectra are similar for Ru PEI in the presence and absence of DNA. Ru PEI/DNA displayed a lifetime of $\tau_{air} = 246$ ns compared to $\tau_{air} = 269$ ns for Ru PEI alone. DNA binding had little effect on the luminescence properties of Ru PEI for the conditions employed.

Prostate cancer (LNCaP) cells were transfected with a plasmid encoding for green fluorescent protein (GFP) using Ru PEI (7900 Da, N/P = 18−54) and L-PEI (N/P = 12) vectors for comparison (Figure 4). Initial N/P ratios explored were based on the results derived from the gel shift assay; however, for better results, these were increased to N/P = 54, a typical range of loadings over which transfection is observed.[17,63] GFP expression was observed for Ru PEI (N/P = 18), and transfection efficiency increased with increasing N/P ratio (Figure 5) with no observed cellular toxicity. However, even at an N/P ratio of 48, the transfection efficiency for Ru PEI was only

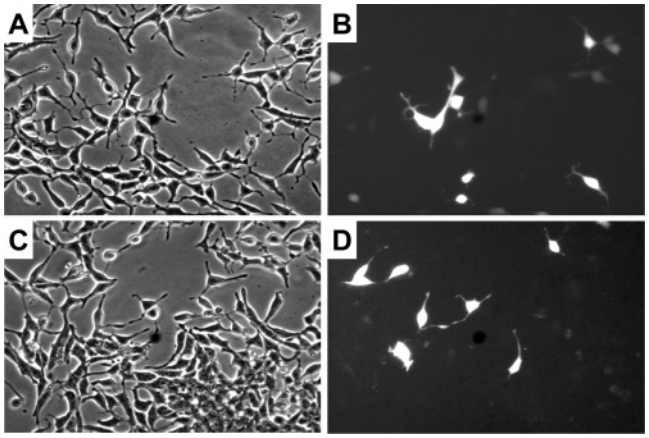

Figure 4. Transfection of LNCaP prostate cancer cells with a plasmid encoding for GFP using L-PEI (22 000 Da, N/P ratio = 12) (A,B) and Ru PEI (7900 Da, N/P ratio = 48) (C,D). After 2 days, cells were fixed with formaldehyde and imaged by brightfield (A,C) and fluorescence (B,D) microscopy (10× magnification), showing total cells and transfected cells, respectively.

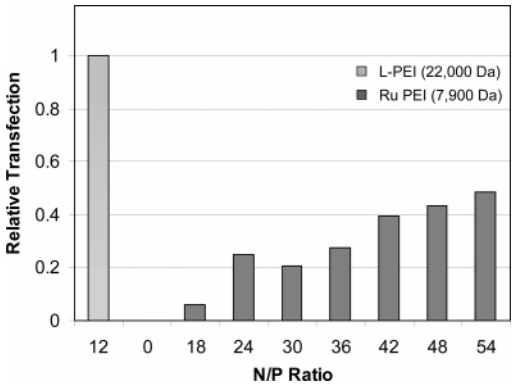

Figure 5. Transfection efficiency for Ru PEI relative to that for L-PEI. Cells were transfected with pGFP (3 μg) and PEI (L-PEI or Ru PEI) complexes at various N/P ratios in 150 mM NaCl.

~50% relative to that for L-PEI. This may be due to the difference in molecular weights and architectures of the PEI vectors employed. Although low molecular weight PEI is less toxic, transfection efficiencies can be lower too.[34] While both branched and L-PEIs effectively entrap DNA, in some cases transfection efficiencies of branched polymers can be lower than those for linear systems,[65−67] though this depends on the cell line and experimental conditions. Additionally, transfection of LNCaP cells can be difficult compared to that of other cell lines because of slow growth and a tendency to form aggregates.[68] Thus, these findings with Ru PEI are consistent with previous reports.

Conclusion

PMCs are versatile multifunctional materials with potential applications as delivery vectors. Living polymerization allows control over polymer architecture and molecular weight, and the metal serves as a modular template for architectural variation and a responsive element in materials. Appropriate material compositions must be targeted and tested if PMCs are to be used in biomedical contexts. Here, Ru PEI-based polymers were generated from Ru PEOX as a model for gene delivery agents with incorporated imaging agents. The effects of polymer composition on luminescence were investigated, and DNA entrapment and delivery were explored. Although the scope of

Ru PEOX synthesis via both living cationic polymerization and macroligand chelation is limited, conversion of Ru PEOX to Ru PEI via acid hydrolysis proceeds relatively smoothly with little chromophore degradation as determined by UV−vis spectroscopy. Spectroscopic analysis reveals red shifts in the absorption and emission spectra and decreases in the emission intensities and luminescence lifetimes for Ru PEI relative to those of Ru PEOX and the nonpolymeric $[Ru(bpy)_3]Cl_2$ parent compound in methanol and aqueous solutions. Further modification of acid or base stable, inert metal chromophores is required for the incorporation of imaging capacity into PEI PMCs via this metalloinitiation route. Coupling strategies may be more amenable to the generation of metal-centered PEI materials. Entrapment of DNA by Ru PEI stars is comparable to linear cationic polymers of higher molecular weight and more efficient than branched PEI materials of similar molecular weight. Transfection of LNCaP prostate cancer cells with GFP was achieved using Ru PEI vectors. Molecular weight, architecture, and cell type effects follow reported trends. This model study serves as a starting point for further adaptation of PMCs for gene delivery and other biomedical applications.

Acknowledgment. We thank the National Science Foundation (BES 0402212 and CHE 0410061), American Cancer Society, Commonwealth Health Research Board, UVA Fund for Excellence in Science and Technology, and the Department of Defense CDMRP (W81XWH-04-1-0112) for support for this research.

References and Notes

(1) Schreier, H. *Pharm. Acta Helv.* **1994**, *68*, 145−159.
(2) Verma, I. M.; Somia, N. *Nature* **1997**, *389*, 239−242.
(3) Neu, M.; Sitterberg, J.; Bakowsky, U.; Kissel, T. *Biomacromolecules* **2006**, *7*, 3428−3438.
(4) Kim, S. H.; Jeong, J. H.; Cho, K. C.; Kim, S. W.; Park, T. G. *J. Controlled Release* **2005**, *104*, 223−232.
(5) Kim, S. H.; Mok, H.; Jeong, J. H.; Kim, S. W.; Park, T. G. *Bioconjugate Chem.* **2006**, *17*, 241−244.
(6) Moffatt, S.; Papasakelariou, C.; Wiehle, S.; Cristiano, R. *Gene Ther.* **2006**, *13*, 761−772.
(7) Germershaus, O.; Merdan, T.; Bakowsky, U.; Behe, M.; Kissel, T. *Bioconjugate Chem.* **2006**, *17*, 1190−1199.
(8) Jeong, J. H.; Lee, M.; Kim, W. J.; Yockman, J. W.; Park, T. G.; Kim, Y. H.; Kim, S. W. *J. Controlled Release* **2005**, *107*, 562−570.
(9) Merdan, T.; Callahan, J.; Petersen, H.; Kunath, K.; Bakowsky, U.; Kopeckova, P.; Kissel, T.; Kopecek, J. *Bioconjugate Chem.* **2003**, *14*, 989−996.
(10) Arnida; Nishiyama, N.; Kanayama, N.; Jang, W.-D.; Yamasaki, Y.; Kataoka, K. *J. Controlled Release* **2006**, *115*, 208−215.
(11) Nori, A.; Kopecek, J. *Adv. Drug Delivery Rev.* **2005**, *57*, 609−636.
(12) Cavallaro, G.; Campisi, M.; Licciardi, M.; Ogris, M.; Giammona, G. *J. Controlled Release* **2006**, *115*, 322−334.
(13) Zhang, J.; Chua, L. S.; Lynn, D. M. *Langmuir* **2004**, *20*, 8015−8021.
(14) Park, T. G.; Jeong, J. H.; Kim, S. W. *Adv. Drug Delivery Rev.* **2006**, *58*, 467−486.
(15) Kim, Y. H.; Park, J. H.; Lee, M.; Kim, Y.-H.; Park, T. G.; Kim, S. W. *J. Controlled Release* **2005**, *103*, 209−219.
(16) Forrest, M. L.; Koerber, J. T.; Pack, D. W. *Bioconjugate Chem.* **2003**, *14*, 934−940.
(17) Neu, M.; Fischer, D.; Kissel, T. *J. Gene Med.* **2005**, *7*, 992−1009.
(18) Banerjee, P.; Weissleder, R.; Bogdanov, A. *Bioconjugate Chem.* **2006**, *17*, 125−131.
(19) Kircheis, R.; Wightman, L.; Wagner, E. *Adv. Drug Delivery Rev.* **2001**, *53*, 341−358.
(20) Pack, D. W.; Hoffman, A. S.; Pun, S.; Stayton, P. S. *Nat. Rev. Drug Discovery* **2005**, *4*, 581−593.
(21) Merdan, T.; Kopecek, J.; Kissel, T. *Adv. Drug Delivery Rev.* **2002**, *54*, 715−758.
(22) Boussif, O.; Lezoulac'h, F.; Zanta, M. A.; Mergny, M. D.; Scherman, D.; Demeneix, B.; Behr, J.-P. *Proc. Natl. Acad. Sci. U.S.A.* **1995**, *92*, 7297−7301.
(23) Klemm, A. R.; Young, D.; Lloyd, J. B. *Biochem. Pharmacol.* **1998**, *56*, 41−46.
(24) Akinc, A.; Thomas, M.; Klibanov, A. M.; Langer, R. *J. Gene Med.* **2005**, *7*, 657−663.
(25) Jones, G. D.; Langsjoen, A.; Neumann, M. M. C.; Zomlefer, J. *J. Org. Chem.* **1944**, *9*, 125−147.
(26) Fischer, D.; Bieber, T.; Li, Y.; Elsasser, H. P.; Kissel, T. *Pharm. Res.* **1999**, *16*, 1273−1279.
(27) Peterson, H.; Martin, A. L.; Stolnik, S.; Roberts, C. J.; Davies, M. C.; Kissel, T. *Macromolecules* **2002**, *35*, 9854−9856.
(28) Akiyama, Y.; Harada, A.; Nagasaki, Y.; Kataoka, K. *Macromolecules* **2000**, *33*, 5841−5845.
(29) Brissault, B.; Kichler, A.; Guis, C.; Leborgne, C.; Danos, O.; Cheradame, H. *Bioconjugate Chem.* **2003**, *14*, 581−587.
(30) Jeong, J. H.; Song, S. H.; Lim, D. W.; Lee, H.; Park, T. G. *J. Controlled Release* **2001**, *73*, 391−399.
(31) Yuan, J.-J.; Jin, R.-H. *Langmuir* **2005**, *21*, 3136−3145.
(32) El-Aneed, A. *J. Controlled Release* **2004**, *94*, 1−14.
(33) Wightman, L.; Kircheis, R.; Rössler, V.; Carotta, S.; Ruzicka, R.; Kursa, M.; Wagner, E. *J. Gene Med.* **2001**, *3*, 362−372.
(34) Godbey, W. T.; Kenneth, K. W.; Antonios, G. M. *J. Biomed. Mater. Res.* **1999**, *45*, 268−275.
(35) Gosselin, M. A.; Guo, W.; Lee, R. J. *Bioconjugate Chem.* **2001**, *12*, 989−994.
(36) Petersen, H.; Fechner, P. M.; Martin, A. L.; Kunath, K.; Stolnik, S.; Roberts, C. J.; Fischer, D.; Davies, M. C.; Kissel, T. *Bioconjugate Chem.* **2002**, *13*, 845−854.
(37) Fraser, C. L.; Smith, A. P. *J. Polym. Sci., Part A: Polym. Chem.* **2000**, *38*, 4704−4716.
(38) Schubert, U. S.; Eschbaumer, C. *Angew. Chem., Int. Ed.* **2002**, *41*, 2892−2926.
(39) Hoogenboom, R.; Schubert, U. S. *Chem. Soc. Rev.* **2006**, *35*, 622−629.
(40) Manners, I. *Synthetic Metal-Containing Polymers*; Wiley VCH: Weinhem, Germany, 2004.
(41) Lamba, J. J. S.; Fraser, C. L. *J. Am. Chem. Soc.* **1997**, *119*, 1801−1802.
(42) McAlvin, J. E.; Fraser, C. L. *Macromolecules* **1999**, *32*, 6925−6932.
(43) Schubert, U.; Nuyken, O.; Hochwimmer, G. *J. Macromol. Sci., Pure Appl. Chem.* **2000**, *37*, 645−658.
(44) Collins, J. E.; Lamba, J. J. S.; Love, J. C.; McAlvin, J. E.; Ng, C.; Peters, B. P.; Wu, X.; Fraser, C. L. *Inorg. Chem.* **1999**, *38*, 2020−2024.
(45) McAlvin, J. E.; Fraser, C. L. *Macromolecules* **1999**, *32*, 1341−1347.
(46) McAlvin, J. E.; Scott, S. B.; Fraser, C. L. *Macromolecules* **2000**, *33*, 6953−6964.
(47) Pangborn, A. B.; Giardello, M. A.; Grubbs, R. H.; Rosen, R. K.; Timmers, F. J. *Organometallics* **1996**, *15*, 1518−1520.
(48) Smith, A. P.; Fraser, C. L. *J. Polym. Sci., Part A: Polym. Chem.* **2002**, *40*, 4250−4255.
(49) Carraway, E. R.; Demas, J. N.; DeGraff, B. A. *Anal. Chem.* **1991**, *63*, 332−336.
(50) Kautsky, H. *Trans. Faraday Soc.* **1939**, *35*, 216−219.
(51) Kem, K. M. *J. Polym. Sci., Part A: Polym. Chem.* **1979**, *17*, 1977−1990.
(52) Smith, A. P.; Fraser, C. L. *Macromolecules* **2003**, *36*, 5520−5525.
(53) Smith, A. P.; Fraser, C. L. *Macromolecules* **2002**, *35*, 594−596.
(54) Corbin, P. S.; Webb, M. P.; McAlvin, J. E.; Fraser, C. L. *Biomacromolecules* **2001**, *2*, 223−232.
(55) Wu, X.; Fraser, C. L. *Macromolecules* **2000**, *33*, 4053−4060.
(56) Wu, X.; Fraser, C. L. *Macromolecules* **2000**, *33*, 7776−7785.
(57) Juris, A.; Balzani, V.; Barigelletti, F.; Campagna, S.; Belser, P.; von Zelewsky, A. *Coord. Chem. Rev.* **1988**, *84*, 85−277.
(58) Cook, M. J.; Lewis, A. P.; McAuliffe, G. S. G.; Skarda, V.; Thomson, A. J.; Glasper, J. L.; Robbins, D. J. *J. Chem. Soc., Perkin Trans. 2* **1984**, 1293−1301.
(59) Lakowicz, J. R. *Principles of Fluorescence Spectroscopy*, 2nd ed.; Kluwer Academic/Plenum Publishers: New York, 1999; p 698.
(60) Vogtle, F.; Plevoets, M.; Nieger, M.; Azzellini, G. C.; Credi, A.; De Cola, L.; De Marchis, V.; Venturi, M.; Balzani, V. *J. Am. Chem. Soc.* **1999**, *121*, 6290−6298.
(61) Bourdelande, J. L.; Font, J.; Marques, G.; Abdel-Shafi, A. A.; Wilkinson, F.; Worrall, D. R. *J. Photochem. Photobiol., A* **2001**, *138*, 65−68.
(62) DeGraff, B. A.; Demas, J. N. In *Reviews in Fluorescence*; Geddes, C., Lakowicz, J. R., Eds.; Springer Science: New York, 2005; Vol. 2, pp 125−151.

(63) Ferrari, S.; Moro, E.; Pettenazzo, A.; Behr, J. P.; Zacchello, F.; Scarpa, M. *Gene Ther.* **1997**, *4*, 1100−1106.
(64) Kunath, K.; von Harpe, A.; Fischer, D.; Peterson, H.; Bickel, U.; Voigt, K.; Kissel, T. *J. Controlled Release* **2003**, *89*, 113−125.
(65) Ahn, C.-H.; Chae, S. Y.; Bae, Y. H.; Kim, S. W. *J. Controlled Release* **2002**, *80*, 273−282.
(66) Peterson, H.; Fechner, P. M.; Fischer, D.; Kissel, T. *Macromolecules* **2002**, *35*, 6867−6874.
(67) Zhong, Z.; Feijen, J.; Lok, M. C.; Hennink, W. E.; Christensen, L. V.; Yockman, J. W.; Kim, Y.-H.; Kim, S. W. *Biomacromolecules* **2005**, *6*, 3440−3448.
(68) Frønsdal, K.; Engedal, N.; Saatcioglu, F. *Prostate (N.Y., NY, U.S.)* **2000**, *43*, 111−117.

BM700481H